Influence of Heat Transform and Rotation of Sutterby Fluid in an Asymmetric Channel

Asmaa A. Mohammed[1,2]*, Liqaa Zeki Hummady[1]

[1]*Department of Mathematics, College of Science, University of Baghdad, Baghdad, Iraq*
[2]*Department of Mathematics, College of Science for Women, University of Baghdad, Baghdad, Iraq*

Abstract:

In this research, the effect of the rotation variable on the peristaltic flow of Sutterby fluid in an asymmetric channel with heat transfer is investigated. The modeling of mathematics is created in the presence of the effect of rotation, using constitutive equations following the Sutterby fluid model. In flow analysis, assumptions such as long wave length approximation and low Reynolds number are utilized. The resulting nonlinear equation is numerically solved using the perturbation method. The effects of the Grashof number, the Hartmann number, the Hall parameter, the magnetic field, the Sutterby fluid parameter, and heat transfer analysis on the velocity and the pressure gradient are analyzed graphically. Utilizing MATHEMATICA software, numerical results are computed. It is discovered that velocity varies with parameters, while the pressure gradient is directly proportional to most parameters.

Keywords: Sutterby fluid, Peristaltic flow, Magnetic field, Heat transfer.

تأثير الانتقال الحراري والدوران لسائل ساتيربي في قناة غير متماثلة

اسماء عبدالحسين محمد*[1,2] ، لقاء زكي حمادي[1]

[1]قسم الرياضيات ، كلية العلوم، جامعة بغداد، بغداد، العراق

[2]قسم الرياضيات ، كلية العلوم للبنات، جامعة بغداد، بغداد، العراق

الخلاصه

في هذا البحث تم دراسة تأثير متغير الدوران على التدفق التمعجي لسائل سوتربي في قناة غير متناظرة مع انتقال الحرارة. يتم إنشاء النمذجة الرياضية في وجود تأثير الدوران، باستخدام المعادلات التأسيسية التي تتبع نموذج سائل سوتربي. في تحليل التدفق، يتم استخدام افتراضات مثل تقريب طول الموجة الطويلة وانخفاض عدد رينولدز. تم حل المعادلة غير الخطية الناتجة عددياً باستخدام طريقة الاضطراب. يتم تحليل تأثيرات رقم كراشوف، ورقم هارتمان، ومعلمة هال، والمجال المغناطيسي، ومعلمة سائل سوتربي، وتحليل نقل الحرارة على السرعة وتدرج الضغط بيانياً. باستخدام برنامج ماثيماتيكا، تم حساب النتائج العددية. تم اكتشاف أن السرعة تختلف باختلاف المعلمات. بينما يتناسب تدرج الضغط تناسباً طردياً مع معظم المعلمات.

1. Introduction

*Email: asmaaaa_math@csw.uobaghdad.edu.iq

A special type of pumping is known as peristaltic pumping, which is a series of contractions and diastoles that push fluid along [1]. Some examples of such physiological processes are the passage of food, chyme, and urine. Peristalsis is the driving force behind everything from worm movement to the transfer of noxious and clean fluids to the operation of finger pumps and the heart-lung machine. Damping, dispensability, and tension in the vasculature play a critical part in physiological processes involving peristalsis, such as blood flow, [2]. Studies of peristalsis were first introduced in [3] and [4]. Since then, researchers have made numerous attempts to dissect the peristaltic movement of fluids and its implications in the medical and business worlds. In biological systems and industrial fluid transport, heat transfer is a fundamental principle. One of the most essential roles of the cardiovascular system is maintaining the body's temperature. Air that enters the lungs must also be tempered to the body's temperature. This is accomplished through the use of all blood vessels. There are three methods of heat transmission; however, convection is the most relevant for fluid circulation in the human body. Human and animal bodies use convection heat transfer to release heat generated by metabolic processes into the environment, [5]. In recent years, research [6-9] has been conducted on the interaction between temperature and mass effects, as well as the influence of variable viscosity and temperature. Researchers investigated the effects of initial pressure and rotation on the peristaltic motion of an incompressible fluid in [10], [11]. Since Abdulhadi [12], Sadaf [13], Abdulla [14] and Akram [15] examined the mechanism of peristaltic transport, which is attracted the interest of numerous researchers. Non-Newtonian fluids are more recognized in many industrial and physiological processes than viscous liquids.Various types of non-Newtonian substances can be usually seen in nature such as ketchup, shampoo, paints, lubricants and blood among that, Sutterby liquid [16] is one of these materials characterizing the ionic high polymer solutions, [17]. Waveform motion of non-Newtonian fluids through porous channels is discussed in [18-21], where the effects of rotation and an inclined MHD are considered. The effects of radiation and convection in a Sutterby fluid are discussed in [22]. In [23], electroosmotic peristaltic transport of Sutterby nanofluids is investigated. The peristaltic flow of a Sutterby liquid in an inclined channel was investigated in [24]. In [17], convection and Hall current were used to simulate the MHD peristaltic transport of a Sutterby nanofluid.

In this paper, we will look at the effects of rotation on heat transfer for peristaltic transport in an asymmetric channel. We will do this by using different values of the parameters of rotation, amplitude wave, and channel taper, as well as different values of the Grashof number, the Hartmann number, and the Hall parameter, based on the changes in velocity, pressure gradient, and heat transfer.

2. *A mathematical formulation for asymmetric flow*

Consider the peristaltic transport of an incompressible Sutterby fluid through a two-dimensional asymmetric conduit that has a width of $(d' + d)$. whereas the motion is steady inside a coordinate system flowing there at wave speed (c) in the wave framer $(\bar{X}, \bar{Y})$.

The geometry of a wall's structure is described as:

$$\overline{h_1}(\bar{X}, \bar{t}) = d - a_1 \sin\left[\frac{2\pi}{\lambda}(\bar{x} - c\bar{t})\right] \tag{1}$$

$$\overline{h_2}(\bar{X}, \bar{t}) = -d' - a_2 \sin\left[\frac{2\pi}{\lambda}(\bar{x} - c\bar{t}) + \Phi\right] \tag{2}$$

In which $\overline{h_1}(\bar{X}, \bar{t})$, $\overline{h_2}(\bar{X}, \bar{t})$ are the lower and upper wall respectively, (d, d') indicates the channel width, (a_1, a_2) are the wave's amplitudes, (λ) represents the wavelength, (c) is the speed of wave, (Φ) varies in the range $(0 \leq \Phi \leq \pi)$, when the value of $\Phi = 0$ the channel is symmetric with waves out of phase and $\Phi = \pi$ waves are in phase the rectangular coordinates

is designed in such a method that $\bar{X} - axis$ is along the path that waves use for propagation and $\bar{Y} - axis$ perpendicular to $\bar{X}$, $\bar{t}$ represents the time.

Further, a_1, a_2, d, d' and Φ satisfy the following condition

$$a_1^2 + a_2^2 + 2a_1a_2 \cos\Phi \le (d + d')^2 \tag{3}$$
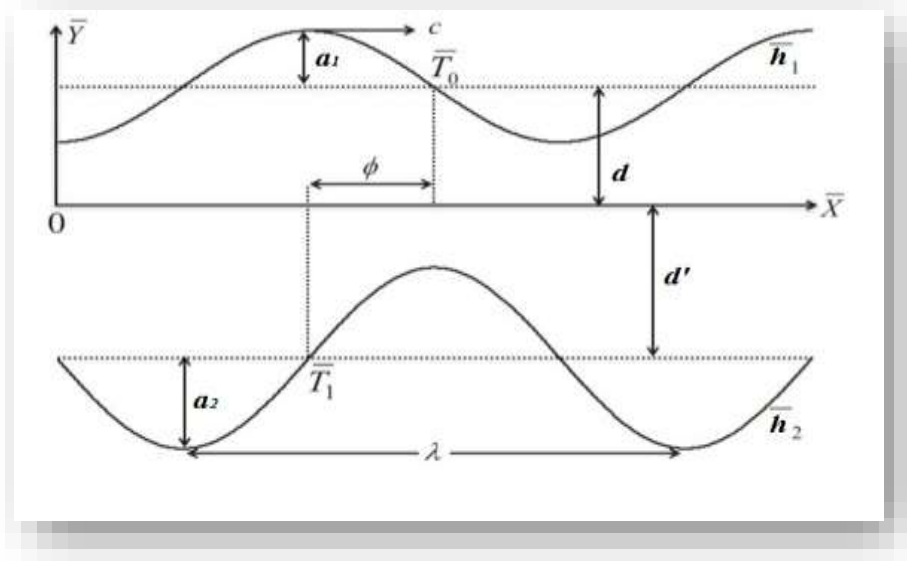
Figure 1: Asymmetric channel coordinates in the Cartesian and Dimensional Systems

3. *Basic equation*

The additional stress tensor for the Sutterby model is determined by [23]:

$$\bar{S} = \frac{\mu}{2}\left[\frac{\sinh^{-1}(n\dot{\gamma})}{n\dot{\gamma}}\right]^{m^*} A_1 \tag{4}$$

$$\dot{\gamma} = \sqrt{\frac{1}{2}\text{tras}(A_1)^2} \tag{5}$$

$$A_1 = \nabla\bar{V} + (\nabla\bar{V})^{\text{T}} \tag{6}$$

Where $\bar{S}$ expresses the extra tensor's stress, n and m^* representing the material constants of the Sutterby fluid, $\nabla = (\partial\bar{X}, \partial\bar{Y}, 0)$ is the gradient vector, μ represents the dynamic viscosity and A_1 represents the first Rivilin–Ericksen tensor. The phrase $\sinh^{-1}$ is approximately equivalent to

$$\sinh^{-1}\left(\frac{\dot{\gamma}}{n}\right) = \frac{\dot{\gamma}}{n} - \frac{\dot{\gamma}^3}{6n^3}, \left|\frac{\dot{\gamma}^5}{6n^5}\right| \ll 1 \tag{7}$$

The constituents of the extra stress tensor of Sutterby that are defined by Eq.(4) are listed as follows:

$$\bar{S}_{\bar{X}\bar{X}} = \frac{\mu}{2}[1 - \frac{mn^2}{6}\left(2\bar{U}_{\bar{X}}^2 + (\bar{V}_{\bar{X}} + \bar{U}_{\bar{Y}})^2 + 2\bar{V}_Y^2\right)]2\bar{U}_{\bar{X}} \tag{8}$$

$$\bar{S}_{\bar{X}\bar{Y}} = \frac{\mu}{2}\left[1 - \frac{mn^2}{6}\left(2\bar{U}_{\bar{X}}^2 + (\bar{V}_{\bar{X}} + \bar{U}_{\bar{Y}})^2 + 2\bar{V}_Y^2\right)\right](\bar{U}_{\bar{X}} + \bar{V}_{\bar{Y}}) \tag{9}$$

$$\bar{S}_{\bar{Y}\bar{Y}} = \frac{\mu}{2}\left[1 - \frac{mn^2}{6}\left(2\bar{U}_{\bar{X}}^2 + (\bar{V}_{\bar{X}} + \bar{U}_{\bar{Y}})^2 + 2\bar{V}_Y^2\right)\right]2\bar{V}_{\bar{Y}} \tag{10}$$

4. *governing equation*

The flow is controlled by three coupled nonlinear partial differentials of continuity, momentum, and energy, the governing equations in frame $(\bar{X}, \bar{Y})$ can be written as follows:

$$\frac{\partial\bar{U}}{\partial\bar{X}} + \frac{\partial\bar{V}}{\partial\bar{Y}} = 0 \tag{11}$$

$$\rho \left(\frac{\partial \overline{U}}{\partial \overline{t}} + \overline{U} \frac{\partial \overline{U}}{\partial \overline{X}} + \overline{V} \frac{\partial \overline{U}}{\partial \overline{Y}} \right) - \rho \Omega \left(\Omega \overline{U} + 2 \frac{\partial \overline{V}}{\partial \overline{t}} \right) = -\frac{\partial \overline{P}}{\partial \overline{X}} + \frac{\partial \overline{S}_{\overline{X}\overline{X}}}{\partial \overline{X}} + \frac{\partial \overline{S}_{\overline{X}\overline{Y}}}{\partial \overline{Y}} - \frac{\sigma B_0{}^2}{(1+m^2)} (\overline{U} - m\overline{V}) + g\,\rho \beta_T (T - T_0) \tag{12}$$

$$\rho \left(\frac{\partial \overline{V}}{\partial \overline{t}} + \overline{U} \frac{\partial \overline{V}}{\partial \overline{X}} + \overline{V} \frac{\partial \overline{V}}{\partial \overline{Y}} \right) - \rho \Omega \left(\Omega \overline{U} - 2 \frac{\partial \overline{U}}{\partial \overline{t}} \right) = -\frac{\partial \overline{P}}{\partial \overline{Y}} + \frac{\partial \overline{S}_{\overline{X}\overline{Y}}}{\partial \overline{X}} + \frac{\partial \overline{S}_{\overline{Y}\overline{Y}}}{\partial \overline{Y}} - \frac{\sigma B_0{}^2}{(1+m^2)} (\overline{V} + m\overline{U}) \tag{13}$$

$$\rho C_P \left(\frac{\partial}{\partial \overline{t}} + \overline{U} \frac{\partial}{\partial \overline{X}} + \overline{V} \frac{\partial}{\partial \overline{Y}} \right) \overline{T} = k \left(\frac{\partial^2}{\partial \overline{t}^2} + \frac{\partial^2}{\partial \overline{X}^2} + \frac{\partial^2}{\partial \overline{Y}^2} \right) \overline{T} + \varphi_0 \tag{14}$$

Where ρ is the fluid density, $(\overline{U}, \overline{V})$ are the velocity components, $\overline{P}$ represents the hydrodynamic pressure, $\overline{S}_{\overline{X}\overline{X}}$, $\overline{S}_{\overline{X}\overline{Y}}$, and $\overline{S}_{\overline{Y}\overline{Y}}$ are the constituents of the extra stress tensor $\overline{S}$. σ is the electrical conductivity, φ_0 is the steady heat addition/absorption, B_0 is an applied magnetic field, β_T is the thermal expansion coefficient, g is the gravitational acceleration and Ω represents the rotation. The specific heat, thermal conductivity and temperature are denoted by C_P, k and $\overline{T}$, respectively. Peristaltic movement in reality is an unstable behavior, but it can be considered to be steady via the change from the experimental frame (fixed frame) $(\overline{X}, \overline{Y})$ to the wave frame (moved frame) $(\overline{x}, \overline{y})$. The following transformations establish the link between coordinates, velocities, and pressure in laboratory frame $(\overline{X}, \overline{Y})$ to wave frame $(\overline{x}, \overline{y})$:

$$\overline{X} = \overline{x} - c\overline{t}, \overline{Y} = \overline{y}, \overline{U} = \overline{u} - c, \overline{V} = \overline{v}, \overline{P}(\overline{X}, \overline{Y}, \overline{t}) = \overline{p}(\overline{x}, \overline{y}) \tag{15}$$

Where $\overline{u}$ and $\overline{v}$ represent the components of velocity, and $\overline{p}$ denotes the pressure in the wave frame. Now, we will substitute Eq.(15) into Eqs.(1), (2), and (11)-(10) and then normalize the equation that is produced by doing so by utilizing the non-dimensional quantities that are listed below:

$$x = \frac{1}{\lambda} \overline{x}, \; y = \frac{1}{d} \overline{y}, \; u = \frac{1}{c} \overline{U}, \; v = \frac{1}{c} \overline{V}, \; P = \frac{d^2}{\lambda \mu c} \overline{P}, \; t = \frac{c}{\lambda} \overline{t}, \; h_1 = \frac{1}{d} \overline{h_1}, \; h_2 = \frac{1}{d} \overline{h_2}, \; \delta = \frac{d}{\lambda}, \; Re = \frac{\rho c d}{\mu}, \; \overline{T} = T - T_0, \; \theta = \frac{T - T_0}{T_1 - T_0}, \; S_{ij} = \frac{d}{\mu c} \overline{S}_{\overline{I}\overline{J}}, \; Gr = \frac{g \beta_T (T - T_0) d^2}{\mu c}, \; Pr = \frac{\mu c_p}{k} \tag{16}$$

Where, (δ) represents the wave number, (h_1) and (h_2) are the non-dimensional upper and lower wall surface, respectively. (Re) is the Reynolds number, (Pr) is the dimensionless Prandtl number, (Gr) is the dimensionless Grashof number, (M) is the Hartman number, (Φ) is the face difference, (δ) is the wave number, and θ is the temperature, (A) is the Sutterby liquid parameter, and (T_0) and (T_1) are the wall temperatures at the top and bottom, respectively. Then, in view of Eq.(16), Eqs.(1), (2), and (11)-(14) take the form :

$$h_1(x) = 1 + a \sin x \tag{17}$$

$$h_2(x) = -d_1 - b \sin (x + \Phi) \tag{18}$$

$$\delta \frac{\partial u}{\partial x} + \frac{\partial v}{\partial y} = 0 \tag{19}$$

$$Re \left(\delta \frac{\partial u}{\partial t} + \delta u \frac{\partial u}{\partial x} + v \frac{\partial u}{\partial y} \right) - \frac{\rho d^2}{\mu} \Omega \left(\Omega u + 2\delta \frac{\partial v}{\partial t} \right) = -\frac{\partial p}{\partial x} + \delta \frac{\partial s_{xx}}{\partial x} + \frac{\partial \overline{s}_{\overline{X}\overline{Y}}}{\partial y} - \frac{\sigma B_0{}^2}{(1+m^2)} (u - mv) + Gr\,\theta \tag{20}$$

$$Re\delta \left(\delta \frac{\partial v}{\partial t} + \delta u \frac{\partial v}{\partial x} + v \frac{\partial v}{\partial y} \right) - Re \frac{d}{c} \Omega \left(\Omega \delta u - 2\delta^2 \frac{\partial u}{\partial t} \right) = -\frac{\partial p}{\partial y} + \delta^2 \frac{\partial s_{xy}}{\partial x} + \delta \frac{\partial s_{yy}}{\partial y} - \frac{\sigma B_0{}^2}{(1+m^2)} \frac{d^2}{\mu} \delta (v + mu) \tag{21}$$

$$RePr\delta \left(\frac{\partial}{\partial t} + u \frac{\partial}{\partial x} + v \frac{\partial}{\partial y} \right) \theta = \left(\delta^2 \frac{c^2 \partial^2}{\partial t^2} + \delta^2 \frac{\partial^2}{\partial x^2} + \frac{\partial^2}{\partial y^2} \right) \theta + B \tag{22}$$

Introduction to fluid flow (ψ) through a relationship:

$$u = \psi_y, v = -\delta \psi_x \tag{23}$$

Substituted Eqs.(23) in Eq.(19) to Eq.(22) respectively,

$$\delta \frac{\partial \psi_y}{\partial x} - \delta \frac{\partial \psi_x}{\partial y} = 0 \tag{24}$$

$$Re\left(\delta \frac{\partial \psi_y}{\partial t} + \delta \psi_y \frac{\partial \psi_y}{\partial x} - \delta \psi_x \frac{\partial \psi_y}{\partial y}\right) - \frac{\rho d^2}{\mu}\Omega\left(\Omega\psi_y + 2\delta\frac{\partial v}{\partial t}\right) = -\frac{\partial p}{\partial x} + \delta \frac{\partial s_{xx}}{\partial x} +$$
$$\frac{\partial s_{xy}}{\partial y} - \frac{\sigma B_0{}^2}{(1+m^2)}(\psi_y + m\delta\psi_x) + Gr\,\theta \tag{25}$$

$$Re\delta\left(\delta\frac{\partial v}{\partial t} + \delta\psi_y\frac{\partial v}{\partial x} + \delta^2\psi_x\frac{\partial \psi_x}{\partial y}\right) - Re\frac{d}{c}\Omega\left(\Omega\delta\psi_y - 2\delta^2\frac{\partial \psi_y}{\partial t}\right) = -\frac{\partial p}{\partial y} + \delta^2\frac{\partial s_{xy}}{\partial x} +$$
$$\delta\frac{\partial s_{yy}}{\partial y} + \frac{\sigma B_0{}^2}{(1+m^2)}\frac{d^2}{\mu}\delta^2(\psi_x + m\psi_y) \tag{26}$$

$$RePr\delta\left(\frac{\partial}{\partial t} + \psi_y\frac{\partial}{\partial x} - \delta\psi_x\frac{\partial}{\partial y}\right)\theta = \left(\delta^2\frac{c^2\partial^2}{\partial t^2} + \delta^2\frac{\partial^2}{\partial x^2} + \frac{\partial^2}{\partial y^2}\right)\theta + B \tag{27}$$

When (Re and $\delta \ll 1$), Eqs.(25)-(27) become in the form:

$$-\frac{\rho d^2}{\mu}\Omega^2\psi_y = -\frac{\partial p}{\partial x} + \frac{\partial s_{xy}}{\partial y} - \frac{M^2}{(1+m^2)}\psi_y + Gr\,\theta \tag{28}$$

$$-\frac{\partial p}{\partial y} = 0 \tag{29}$$

$$\frac{\partial^2\theta}{\partial y^2} + B = 0 \tag{30}$$

While an additional stress tensor component takes the following form:

$$s_{xy} = \frac{1}{2}\frac{\partial^2\psi}{\partial y^2} - \frac{A}{2}\left(\frac{\partial^2\psi}{\partial y^2}\right)^3, s_{xx} = 0, s_{yy} = 0 \tag{31}$$

Where $M = \sqrt{\frac{\sigma}{\mu}}B_0 d$ the Hartman number, $A = \frac{mb^2c^2}{6d^2}$ the Sutterby liquid parameter and

$B = \frac{d^2\theta}{k(T_1-T_0)}$ the constant heat radiation

If we substitute equation Eqs.(31) into Eq.(28), then to eliminate the pressure take derivation of Eq.(28) with respect to y, we obtain the following equation:

$$\frac{1}{2}\frac{\partial^4\psi}{\partial y^4}\left[1 - 3A\left(\frac{\partial^2\psi}{\partial y^2}\right)^2\right] - 3A\frac{\partial^2\psi}{\partial y^2}\left(\frac{\partial^3\psi}{\partial y^3}\right)^2 - \left(\frac{M^2}{m^2+1} - \frac{\rho d^2}{\mu}\Omega^2\right)\frac{\partial^2\psi}{\partial y^2} + Gr\frac{\partial\theta}{\partial y} = 0 \tag{32}$$

$$\frac{\partial^2\theta}{\partial y^2} + B = 0 \tag{33}$$

In wave frames, the dimensionless boundary conditions are:

$$\psi = \frac{F}{2}, \frac{\partial\psi}{\partial y} = -1 \; at \; y = h_1 \tag{34}$$

$$\psi = \frac{-F}{2}, \frac{\partial\psi}{\partial y} = -1 \; at \; y = h_2 \tag{35}$$

$$\theta = 0 \; at \; y = h_1, \theta = 1 \; at \; y = h_2 \tag{36}$$

Where F is just the flow rate, which is dimensionless in time in the frame of the wave. It is associated with the form that has no dimensions temporal flow rate Q_1 in the experimental frame via the expression:

$$Q_1 = F + 1 + d \tag{37}$$

as a, b, Φ and d achieve Eq.(3):

$$a^2 + b^2 + 2abcos(\Phi) \le (1 + d_1)^2 \tag{38}$$

Initially, we solve the nonlinear equation Eq.(33) by integral and substituting the boundary conditions Eqs.(36), and then we obtain:

$$\theta = -\frac{-2h_1 + h_1^2h_2B - h_1h_2^2B}{2(h_1-h_2)} - \frac{(2-h_1^2B+h_2^2B)y}{2(h_1-h_2)} - \frac{By^2}{2} \tag{39}$$

Now, we can get the following nonlinear equation by differentiating the equation Eq.(39) with respect to y and substituting it in Eq.(32), we get high nonlinear equation:

$$\frac{\partial^4 \psi}{\partial y^4}\left[1 - 3A\left(\frac{\partial^2 \psi}{\partial y^2}\right)^2\right] - 6A\frac{\partial^2 \psi}{\partial y^2}\left(\frac{\partial^3 \psi}{\partial y^3}\right)^2 - 2\left(\frac{M^2}{m^2+1} - \frac{\rho d^2}{\mu}\Omega^2\right)\frac{\partial^2 \psi}{\partial y^2} +$$
$$2Gr\left(-\frac{(2-h_1^2 B + h_2^2 B)}{2(h_1-h_2)} - By\right) = 0 \tag{40}$$

5. *Solution of the problem*

It is not possible to construct a solution in closed form for each and every one of the arbitrary parameters involved in Eq.(40), as it is highly non-linear and convoluted. Therefore, we use the perturbation approach to get the answer. We expand the solution to include perturbation: [14]

$$\psi = \psi_0 + A\psi_1 + o(A^2) \tag{41}$$

And by substituting the boundary conditions Eq.(34) and Eq.(35) into Eq.(28)-(33) and equating the coefficients of similar powers of A, we obtain the following system of equations:

3.1 Zeroth order system

When such terms of order (A) in a zero-order system are negligible, we obtain

$$\psi_{0yyyy} - \zeta\psi_{0yy} - \gamma y + \eta = 0 \tag{42}$$

Where $\zeta = 2\left(\frac{M^2}{m^2+1} - \frac{\rho d^2}{\mu}\Omega^2\right)$

$\gamma = 2GrB$

And $\eta = 2Gr\left(-\frac{(2-h_1^2 B + h_2^2 B)}{2(h_1-h_2)} - By\right)$

Such that

$$\psi_0 = \frac{F_0}{2}, \frac{\partial \psi_0}{\partial y} = -1 \; at \; y = h_1 \tag{43}$$

and

$$\psi_0 = \frac{-F_0}{2}, \frac{\partial \psi_0}{\partial y} = -1 \; at \; y = h_2 \tag{44}$$

3.2   First order system

$$\psi_{1yyyy} - \zeta\psi_{1yy} = 3\psi_{0yyyy}(\psi_{0yy})^2 + 6\psi_{0yy}(\psi_{0yyy})^2 \tag{45}$$

$$\psi_1 = \frac{F_1}{2}, \frac{\partial \psi_1}{\partial y} = -1 \; at \; y = h_1 \tag{46}$$

and

$$\psi_1 = \frac{-F_1}{2}, \frac{\partial \psi_1}{\partial y} = -1 \; at \; y = h_2 \tag{47}$$

Solving the relevant zeroth-order and first-order systems yields the final stream function equation.

$$\psi = \psi_0 + A\psi_1 \tag{48}$$

6. *Results and discussions*

This section consists of two subsections. Using MATHEMATICA, the velocity distribution is depicted in the first and the pressure gradient is presented in the second.

4.1 Velocity distribution u:

For changing values of u, it reflects the variation in axial velocity throughout the channel. The influence of different values on axial velocity u is introduced in Figurer 2-8 to show the effect of changing the values of $\Omega, M, Gr, m, A, \phi \; and \; B$ on axial velocity u. Figurer 2, we can see that as the rotation (Ω) goes up, the axial velocity decreases on the left side of the wall while increasing along the middle toward the right of the channel walls. Figure , shows that as the Hartmann number (M) goes up, the axial velocity drops in the middle of the channel while increasing near the edge of the channel wall. As illustrated in Figure , the axial velocity reduces near the left and central region of the channel wall as the thermal Grashof number (Gr) increases, while it rises beside the right wall. As shown in Figure , increasing the value of the Hall parameter (m) doesn't change the axial speed. As illustrated in Figure, the axial velocity is

increased in the middle of the channel as the fluid parameter (A) increases, whereas it decreases near the channel wall. Figure shows that raising the face difference (ϕ) decreases the axial velocity near the left wall of the channel but has no effect in the center and along the right wall. As seen in Figure 8, As the constant heat radiation (B) increases, as the constant heat radiation (B) increases, the axial velocity also increases along the wall of the channel.
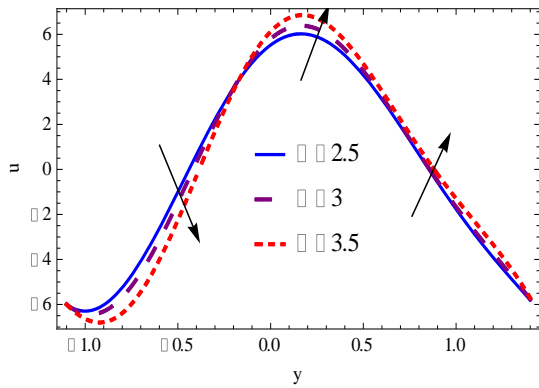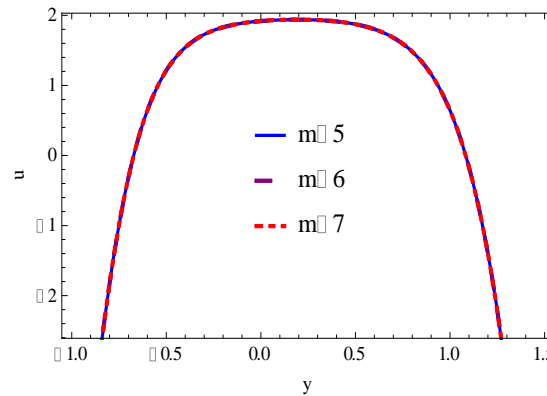

Figurer 2: *Change of velocity in relation to diverse values of Ω when M=0.2, Gr=1, m=5, A=5, ϕ=Pi/6, a=0.5, b=0.1*
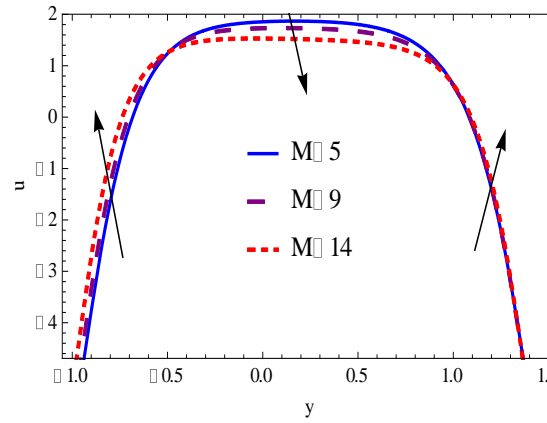
Figure 3: *Change of velocity in relation to diverse values of M when Ω=10, Gr=1, m=5, A=5, ϕ=Pi/6, a=0.5, b=0.1*
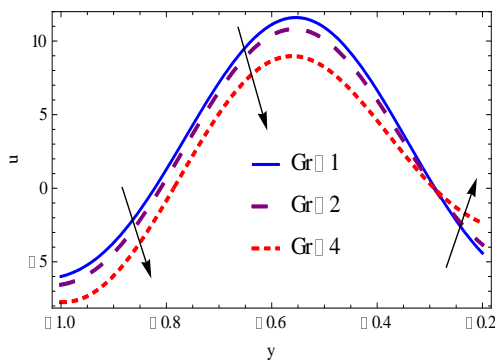
Figure 4: *Change of velocity in relation to diverse values of Gr when Ω=10, M=0.2, m=5, A=5, ϕ=Pi/6, a=0.5, b=0.1*

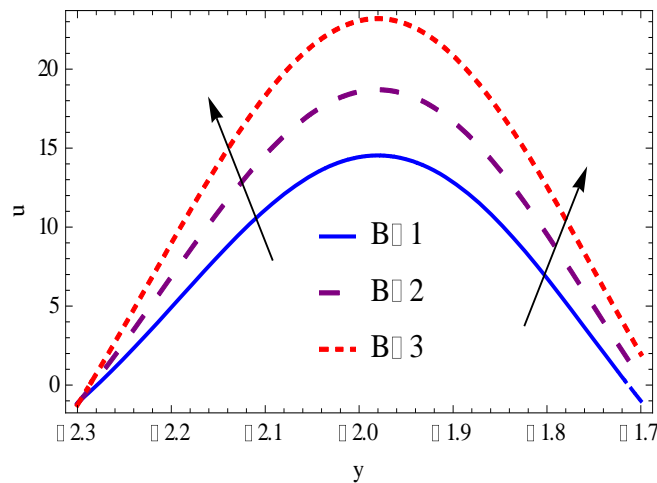**Figure 5:** *Change of velocity in relation to diverse values of m when Ω=10, M=0.2, Gr=1, A=5, ϕ=Pi/6, a=0.5, b=0.1*
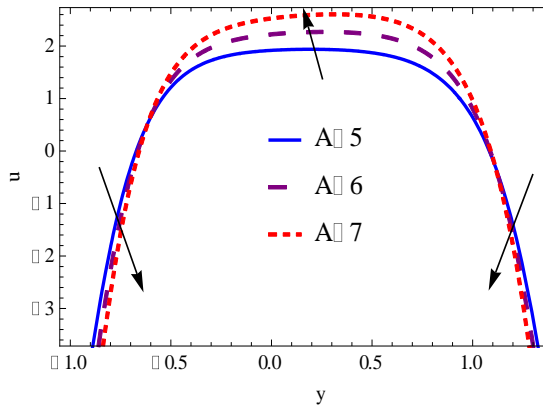
Figure 6: *Change of velocity in relation to diverse values of A when Ω=10, M=0.2, Gr=1, m=5,φ=Pi/6, a=0.5, b=0.1*
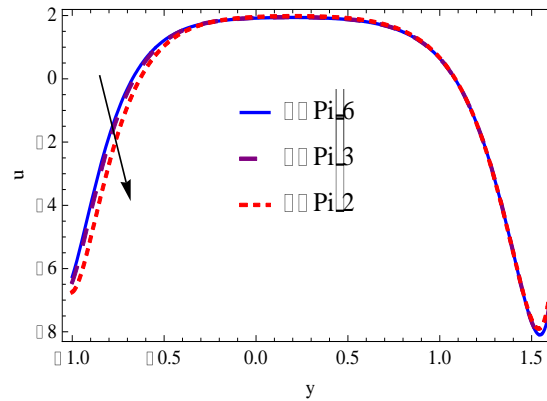
Figure 7: *Change of velocity in relation to diverse values of φ when Ω=10, M=0.2, Gr=1, m=5, A=5, a=0.5, b=0.1*

**Figure 8:** *Change of velocity in relation to diverse values of B when Ω=10,M=0.2,Gr=1,m=5,A=5, φ=Pi/6,a=0.5,b=0.1*
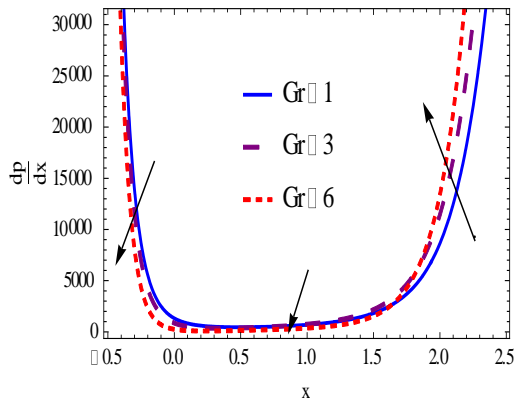
4.2 Pressure gradient dp/dx:

Graphically, the influence that relevant parameters have on the pressure gradient dp/dx can be seen in Figure -Figure . As seen in Figure , increasing the rotation (Ω) results in an increasing pressure gradient. Figure illustrates how increasing values of the Hartmann number (M) are associated with a diminishing pressure gradient. Increasing the thermal Grashof number (Gr) lessens the pressure gradient towards the channel's left edge and the center of the channel but increases it toward the right wall of the channel, as depicted in Figure . Figure 3 demonstrates that the pressure gradient grows as the Hall parameter value (m) increases. Figure 4 shows that the pressure gradient rises as the value of a fluid parameter (A) increases. Figure displays that the pressure gradient reduces towards the left wall in the channel as the face difference (φ) increases whereas there is no influence in the central region and the pressure gradient increases near the right wall. Figure shows that as the constant heat radiation (B) goes up, the pressure gradient goes up.
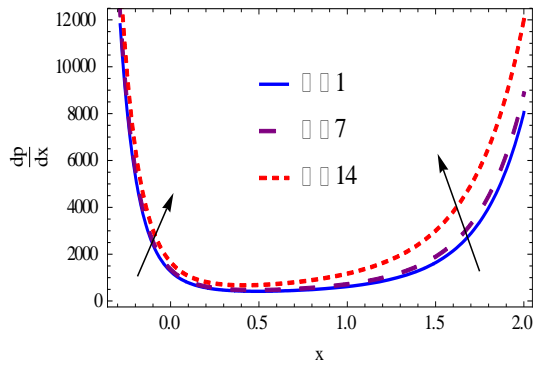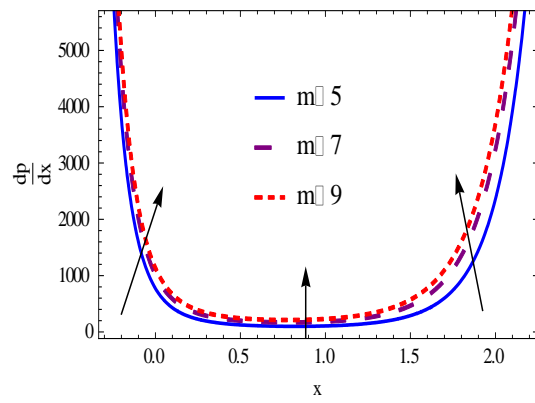
Figure 9*: Change of pressure gradient in relation to diverse values of Ω when M=5,Gr=1,m=7,A=5,ϕ=Pi/6,a=0.7,b=0.8*
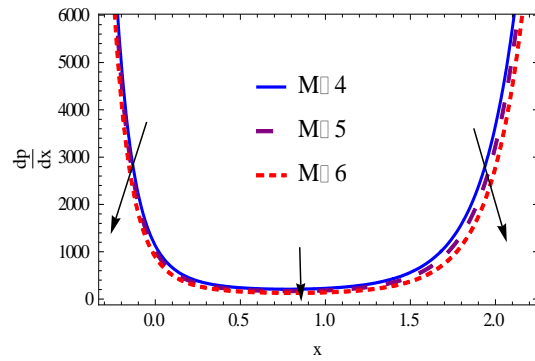
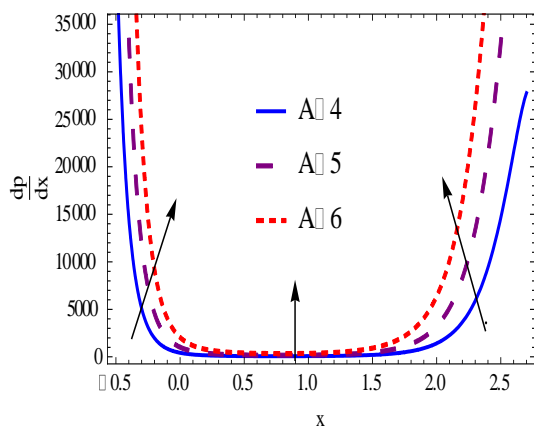**Figure 10***: Change of pressure gradient in relation to diverse values of M when Ω=6,Gr=1,m=7,A=5,ϕ=Pi/6,a=0.7,b=0.8*

Figure 11*: Change of pressure gradient in relation to diverse values of Gr when Ω=6, M=5, m=7, A=5, ϕ=Pi/6, a=0.7, b=0.8*

Figure 3*: Change of pressure gradient in relation to diverse values of m when Ω=6, M=5, Gr=1, A=5, ϕ=Pi/6, a=0.7, b=0.8*

Figure 43*: Change of pressure gradient in relation to diverse values of A when Ω=6, M=5, Gr=1, m=7, ϕ=Pi/6, a=0.7, b=0.8*

Figure 14: *Change of pressure gradient in relation to diverse values of ϕ when Ω=6, M=5, Gr=1, m=7, A=5, a=0.7, b=0.8*

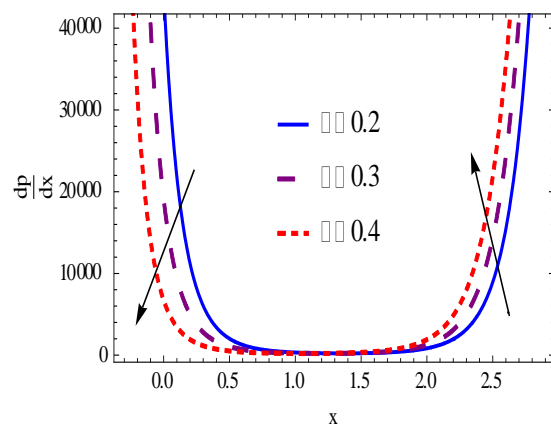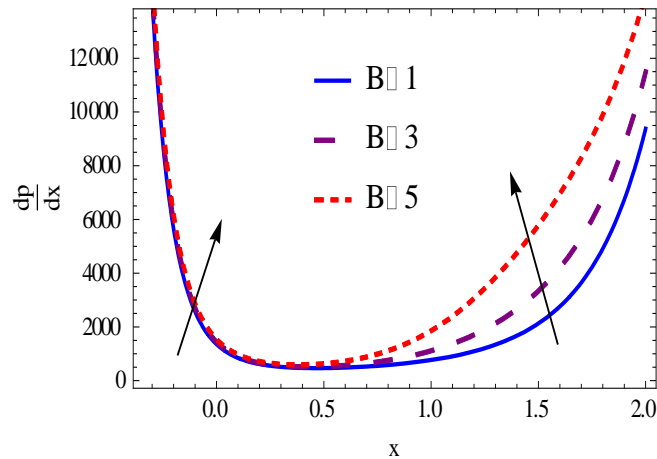**Figure 15***: Change of pressure gradient in relation to diverse values of a when Ω=6, M=5 ,Gr=1, m=7, A=5, ϕ=Pi/6, b=0.8*

7. Conclusion

In this article, we study the influence of heat transfer and rotation of Sutterby fluid in an asymmetric channel. In this investigation, a lot of attention has been paid to the analysis of things like velocity distribution and pressure gradient based on a simple analytical solution. The key consequences of the current study are summarized below:

1. As the rotation (Ω) goes up, the axial velocity decreases on the left side of the wall while it increases along the middle toward the right of the channel walls.

2. In the central part of the channel, the axial velocity reduces as (M) is increased, whereas the axial velocity is increased at the boundaries.

3. The axial velocity reduces near the left and the central region of the channel wall as the thermal Grashof number (Gr) increases, while it rises beside the right wall.

4. There is no effect on the axial velocity with increase in the value (m).

5. The axial velocity is increased in the middle of the channel as (A) increases, whereas it reduces near the channel walls.

6. Increasing (ϕ) decreases the axial velocity at the left wall of the channel, but has no effects on the axial velocity in the middle region or on the right wall.

7. As the constant heat radiation (B) increases, the axial velocity also increases along the wall of the channel.

8. As (Ω), (m), (A), and (B) values increase, the pressure gradient increases.

9. As (M) value increases, the pressure gradient reduces.

10. Increasing the thermal Grashof number (Gr) lessens the pressure gradient towards the channel's left edge and the center of the channel, but has increased toward the right wall of the channel.

11. We can see that as (ϕ) goes up, the pressure gradient goes down near the left side of the channel, stays the same in the middle, and goes up near the right side.

When the rotation is deleted, the work was compared with [2] and the results are compared with high accuracy, and the role of the impact on the issue is clear, as found in the above conclusions.

References:
[1] L. Z. Hummady, "Effect of Couple Stress on Peristaltic Transport of Powell-Eyring Fluid Peristaltic flow in Inclined Asymmetric Channel with Porous Medium," *Wasit Journal of Computer and Mathematics Sciences*, vol. 1, no. 2, pp. 106–118, 2022.
[2] T. Hayat, S. Ayub, A. Alsaedi, A. Tanveer, and B. Ahmad, "Numerical simulation for peristaltic activity of Sutterby fluid with modified Darcy's law," *Results in physics*, vol. 7, pp. 762–768, 2017.

[3] T. W. Latham, "Fluid motions in a peristaltic pump." Massachusetts Institute of Technology, 1966.

[4] A. H. Shapiro, M. Y. Jaffrin, and S. L. Weinberg, "Peristaltic pumping with long wavelengths at low Reynolds number," *Journal of Fluid Mechanics*, vol. 37, no. 4, pp. 799–825, 1969.

[5] H. N. Mohaisen and A. M. Abedulhadi, "Effects of the Rotation on the Mixed Convection Heat Transfer Analysis for the Peristaltic Transport of Viscoplastic Fluid in Asymmetric Channel," *Iraqi Journal of Science*, pp. 1240–1257, 2022.

[6] A. B. Huda, N. S. Akbar, O. A. Beg, and M. Y. Khan, "Dynamics of variable-viscosity nanofluid flow with heat transfer in a flexible vertical tube under propagating waves," *Results in physics*, vol. 7, pp. 413–425, 2017.

[7] H. S. Lew, Y. C. Fung, and C. B. Lowenstein, "Peristaltic carrying and mixing of chyme in the small intestine (an analysis of a mathematical model of peristalsis of the small intestine)," *Journal of Biomechanics*, vol. 4, no. 4, pp. 297–315, 1971.

[8] M. Kothandapani, J. Prakash, and V. Pushparaj, "Analysis of heat and mass transfer on MHD peristaltic flow through a tapered asymmetric channel," *The Journal of Fluids Engineering*, vol. 2015, 2015.

[9] W. S. Khudair and H. H. Dwail, "Studying the magnetohydrodynamics for williamson fluid with varying temperature and concentration in an inclined channel with variable viscosity," *Baghdad Science Journal*, vol. 18, no. 3, 2021, doi: 10.21123/BSJ.2021.18.3.0531.

[10] A. M. Abd-Alla, S. M. Abo-Dahab, and H. D. El-Shahrany, "Effects of rotation and initial stress on peristaltic transport of fourth grade fluid with heat transfer and induced magnetic field," *Journal of Magnetism and Magnetic Materials*, vol. 349, pp. 268–280, 2014.

[11] A. W. Salih and S. B. Habeeb, "Influence Of Rotation, Variable Viscosity And Temperature On Peristaltic Transport In An Asymmetric Channel," *Turkish Journal of Computer and Mathematics Education*, vol. 12, no. 6, pp. 1047–1059, 2021.

[12] A. M. Abdulhadi and T. S. Ahmed, "Effect of magnetic field on peristaltic flow of Walters' B fluid through a porous medium in a tapered asymmetric channel," *Journal of Advances in Mathematics*, vol. 1, no. 12, pp. 6889–6893, 2017.

[13] H. Sadaf, M. U. Akbar, and S. Nadeem, "Induced magnetic field analysis for the peristaltic transport of non-Newtonian nanofluid in an annulus," *Mathematics and Computers in Simulation*, vol. 148, pp. 16–36, 2018.

[14] S. A. Abdulla and L. Z. Hummady, "Inclined magnetic field and heat transfer of asymmetric and porous medium channel on hyperbolic tangent peristaltic flow," *International Journal of Nonlinear Analysis and Applications*, vol. 12, no. 2, pp. 2359–2373, 2021, doi: 10.22075/ ijnaa. 2021.5382.

[15] S. Akram and S. Nadeem, "Influence of induced magnetic field and heat transfer on the peristaltic motion of a Jeffrey fluid in an asymmetric channel: closed form solutions," *Journal of Magnetism and Magnetic Materials*, vol. 328, pp. 11–20, 2013.

[16] J. L. Sutterby, "Laminar converging flow of dilute polymer solutions in conical sections: Part I. Viscosity data, new viscosity model, tube flow solution," *American Institute of Chemical Engineers*, vol. 12, no. 1, pp. 63–68, 1966.

[17] T. Hayat, Z. Nisar, A. Alsaedi, and B. Ahmad, "Analysis of activation energy and entropy generation in mixed convective peristaltic transport of Sutterby nanofluid," *Journal of Thermal Analysis and Calorimetry*, vol. 143, no. 3, pp. 1867–1880, 2021.

[18] T. S. Alshareef, "Impress of rotation and an inclined MHD on waveform motion of the non-Newtonian fluid through porous canal," in *Journal of Physics: Conference Series*, 2020, vol. 1591, no. 1, p. 12061.

[19] K. Kalyani and S. R. MVVNL, "A Numerical Study on Cross Diffusion Cattaneo-Christov Impacts of MHD Micropolar Fluid Across a Paraboloid," *Iraqi Journal of Science*, pp. 1238–1264, 2021.

[20] R. S. Kareem and A. M. Abdulhadi, "Impacts of Heat and Mass Transfer on Magneto Hydrodynamic Peristaltic Flow Having Temperature-dependent Properties in an Inclined Channel Through Porous Media," *Iraqi Journal of Science*, pp. 854–869, 2020.

[21] R. S. Kareem and A. M. Abdulhadi, "Effect of MHD and Porous Media on Nanofluid Flow with Heat Transfer : Numerical Treatment," *Journal of Advanced Research in Fluid Mechanics and Thermal Sciences*, vol. 2, no. 2, pp. 317–328, 2019.

[22] S. Ahmad, M. Farooq, M. Javed, and A. Anjum, "Double stratification effects in chemically reactive squeezed Sutterby fluid flow with thermal radiation and mixed convection," *Results in*

physics, vol. 8, pp. 1250–1259, 2018.

[23] K. Ramesh and J. Prakash, "Thermal analysis for heat transfer enhancement in electroosmosis-modulated peristaltic transport of Sutterby nanofluids in a microfluidic vessel," *Journal of Thermal Analysis and Calorimetry*, vol. 138, no. 2, pp. 1311–1326, 2019.

[24] F. Atlas, M. Javed, and N. Imran, "Effects of heat and mass transfer on the peristaltic motion of Sutterby fluid in an inclined channel," *Multidiscipline Modeling in Materials and Structures*, vol. 16, no. 6, pp. 1357–1372, 2020.